

# Automatic Hippocampus Segmentation from Brain MRI Images

Xiangbo LIN<sup>\*,†</sup>, Tianshuang QIU<sup>\*</sup>, Frédéric Nicolier<sup>†</sup>, Su RUAN<sup>†</sup>

*(\*.Department of Electronic Engineering, Dalian University of Technology, Dalian 116024, China;*

*†. Dept. GE&II, IUT de Troyes, Université de Reims Champagne. Ardnne, 10026 Troyes Cedex, France)*

**Abstract:** Since hippocampal volume measurement is often used in studying Alzheimer's disease to assess disease progression, automatic hippocampus segmentation is an important task in clinical applications. However, it is a challenging task due to its small size, complex shape, fuzzy boundaries, partial volume effects, and anatomical variability. In this paper we propose a new registration method to segment the hippocampus from brain MRI images automatically. It uses a combination of local affine transformation and optical flow based non-rigid registration, which has the advantages of modifying the larger geometric deformation and intensity differences simultaneously. Meanwhile the residual subtle differences decrease due to the high degree of freedom. Quantitative evaluation with respect to manual segmentation is performed on 10 subjects with the spatial overlap (KI value) as the evaluation criterion. The average KI with the proposed method is 0.7749, while it is 0.5811 with another semi-automatic method, ITK-SNAP. It is indicated that the proposed method is more accurate and will be a good choice for hippocampus segmentation.

**Key words:** Hippocampal segmentation; Non-rigid registration; MRI;

## 1. Introduction

In recent years, the analysis of anatomical structures from medical images develops rapidly [1][2][3] due to the widespread research on brain functions and brain disorders. Brain internal structures play a central role in the intellectual capabilities of the human brain. Additionally, these structures are also relevant to a set of clinical conditions, such as Alzheimer's disease. Alzheimer's disease (AD) is the most common cause of dementia worldwide. As the world's population ages, the number of people with Alzheimer's disease has a large increase. AD therefore presents an increasing socio-economic burden with each person affected representing both great personal loss and increased economic cost [4]. A large number of studies have shown that hippocampal volume is lower in AD subjects [5][6]. Since hippocampal volume change is usually expressed as a percentage loss per year, volume measurement of the probable AD will be useful in tracking disease progression or specific disease-related effects of treatment.

However, segmenting brain internal structures remains a challenging task due to their small size, partial volume effects, anatomical variability, and the lack of clearly defined edges [7]. Therefore manual delineation has been used for most MRI-based hippocampal volume studies [5][8] and this is currently considered to be the gold standard for hippocampal measurement. However, manual segmentation is both time consuming and requires trained operators in large studies and clinical trials. Therefore it is necessary to find accurate automatic segmentation methods close to manual delineation.

A variety of computer-assisted methods has been studied to automatically segment brain internal structures of which the hippocampus is one [9]. We can cite deformable models or active contour evolution based methods [10][11][12][13][14], which can be good solutions to the problem because of their abilities to capture the information of

the shapes or structures of interest. However the initialization of these methods prior to deformation remains difficult. Another crucial technology is image registration [1][2][15][16][17]. These methods rely on a reference image volume in which structures of interest have been carefully segmented by experts. To segment a new image volume, a transformation that registers the reference volume to the target volume is computed, which gives a spatial correspondence between the two image volumes. Then regions labeled in the reference volume can be projected onto the volume of interest. The key of this approach is to design a method being capable of computing the transformation in a reliable and accurate way. These methods take advantage of the prior knowledge, which is explicitly provided by the atlas (segmented reference volume), such as structure shape, relative positions between the structures. This allows helping the segmentation of the anatomical structures without clearly defined contours, which motivates the present work.

The adopted method in this paper, Demons registration [18], belongs to intensity based non-rigid registration algorithm. It has high ability to model local deformation and has been used in medical image registration [18][19][20][21] successfully. However the requirements of intensity correspondence and small initial deformation between homologous structures put some limitations on it. In general global rigid or affine transformation and simple histogram match were often used to solve the problem [1][22][23][24][25], but they were not ideal solutions. Therefore, we propose to implement the preprocess using a local affine transformation methods, which has the advantages of modifying the larger geometric deformation and intensity differences simultaneously [26]. Then the Demons registration with higher degree of freedom is used to cope with the residual subtle differences.

## 2. Methods

### 2.1 Intensity and spatial normalization

The designed model of the local affine transformation to get the intensity match and the rough spatial match is

$$m_7 f(x, y, t) + m_8 = f(m_1 x + m_2 y + m_5, m_3 x + m_4 y + m_6, t - 1) \quad (1)$$

Where  $m_i, i = 1, \dots, 6$  are position parameters,  $m_7, m_8$  are brightness and contrast parameters, and a temporal parameter  $t$  is used to distinguish the two images. This model has the advantages that not only the geometric shape and image intensity can be modified simultaneously, but also larger deformation problems can be solved effectively. This is just to meet the needs of the Demons algorithm and enables it a perfect option for preprocessing. The error function is

$$E(\bar{m}) = \sum_{x, y \in \omega} [m_7 f(x, y, t) + m_8 - f(m_1 x + m_2 y + m_5, m_3 x + m_4 y + m_6, t - 1)]^2 \quad (2)$$

Where  $\omega$  denotes a small spatial neighborhood. By minimizing Equation (2), the expected optimized model parameters can be obtained. Since the error function is nonlinear with respect to its unknown parameters, it is unable to get its analytical solutions. Therefore, the error function is approximated using its first-order truncated Taylor series expansion, which is

$$\begin{aligned} E(\bar{m}) &\approx \sum_{x, y \in \omega} \{m_7 f(x, y, t) + m_8 - [f(x, y, t) + f_x(m_1 x + m_2 y + m_5 - x) + f_y(m_3 x + m_4 y + m_6 - y) - f_t]\}^2 \\ &= \sum_{x, y \in \omega} [(f_t - f + x f_x + y f_y) - (x f_x m_1 + y f_x m_2 + x f_y m_3 + y f_y m_4 + f_x m_5 + f_y m_6 - m_7 f - m_8)]^2 \end{aligned} \quad (3)$$

The vector form is

$$E(\bar{m}) = \sum_{x,y \in \omega} [k - \bar{c}^T \bar{m}]^2 \quad (4)$$

Where  $k = f_t - f + xf_x + yf_y$ ,  $\bar{c} = [xf_x \quad yf_x \quad xf_y \quad yf_y \quad f_x \quad f_y \quad f \quad -1]^T$ . Now the error function can be easily minimized analytically by differentiating with respect to the unknown parameters and yields the solutions

$$\bar{m} = \left[ \sum_{x,y \in \omega} \bar{c} \bar{c}^T \right]^{-1} \left[ \sum_{x,y \in \omega} \bar{c} k \right] \quad (5)$$

To guarantee the invertible attributes of the first term in equation (5), the local affine and contrast/brightness parameters in equation (4) should be defined over a large enough spatial neighborhood with sufficient image content. However, according to equation (4), the local affine and contrast/brightness parameters are assumed to be constant over a small spatial neighborhood. So there should be a tradeoff in choosing the size of the neighborhood or an alternative smoothness constraint should be added to make the assumption reasonable. The modified error function in this way is

$$E(\bar{m}) = E_b(\bar{m}) + E_s(\bar{m}) \quad (6)$$

Where  $E_b(\bar{m}) = [k - \bar{c}^T \bar{m}]^2$ ,  $E_s(m) = \sum_{i=1}^8 \lambda_i \left[ \left( \frac{\partial m_i}{\partial x} \right)^2 + \left( \frac{\partial m_i}{\partial y} \right)^2 \right]$  which embodies the smoothness constraint.

The derivative of  $E(\bar{m})$  with respect to the model parameters is

$$\frac{dE(\bar{m})}{d\bar{m}} = -2\bar{c}[k - \bar{c}^T \bar{m}] + 2L[\bar{\bar{m}} - \bar{m}] \quad (7)$$

where,  $\bar{\bar{m}}$  is the component-wise average of  $\bar{m}$  over a small spatial neighborhood,  $\lambda_i$  is a positive constant that controls the relative weight given to the smoothness constraint on parameter  $m_i$ , and  $L$  is a  $8 \times 8$  diagonal matrix with diagonal elements  $\lambda_i$ , and zero off the diagonal. Setting  $dE(\bar{m})/d\bar{m} = 0$  yields the iterative solution for parameters  $\bar{m}$

$$\bar{m}^{(j+1)} = (\bar{c} \bar{c}^T)^{-1} (\bar{c} k + L \bar{\bar{m}}^{(j)}) \quad (8)$$

After preprocess, a rough match is acquired. Then subtle differences are corrected using the Demons registration algorithm.

## 2.2 Non-rigid registration

The main idea of the Demons registration algorithm is to consider the non-rigid registration as a diffusion process. Proper ‘gatekeepers’ are put into in the target image  $S$ , which have the same roles as ‘demons’ in thermodynamics. The source image  $M$  is considered as a deformable grid, in which each vertex is labeled with ‘inside’ and ‘outside’. The polarity of each grid vertex is related with its intensity, which determines the orientation of the force in this point.

Suppose the intensity of each Demons point  $p$  in  $S$  is  $s(p) = I$ , and the intensity of the corresponding point in

$M$  is  $m(p)$ ,  $p$  is labeled outside and its force orientation is according to  $-\nabla s$  if  $m(p) < I$ ; Otherwise, it is labeled inside and its force orientation is according to  $+\nabla s$ .  $M$  deformed continuously until it was as similar as  $S$ .

Demons algorithm is a general scheme and can be applied to many fields by varying its variants. In this paper we focus on medical image registration and the suggested suitable combination [18] is: (1) All pixels of  $S$  are ‘demons’; (2)  $T$  is a free form deformation, smoothed by a Gaussian filter; (3) Linear interpolation method; (4) The Demons force is based on optical flow field theory. The assumption in optical flow field is intensity preservation in image moving process, that is:

$$I(x(t), y(t), z(t), t) = \text{const} \quad (9)$$

The differential is

$$\frac{\partial I}{\partial x} \frac{\partial x}{\partial t} + \frac{\partial I}{\partial y} \frac{\partial y}{\partial t} + \frac{\partial I}{\partial z} \frac{\partial z}{\partial t} = - \frac{\partial I}{\partial t} \quad (10)$$

Let the moving time to be unit time, then

$$\vec{v} \cdot \nabla s = m - s \quad (11)$$

Where  $\vec{v} = (\partial x / \partial t, \partial y / \partial t, \partial z / \partial t)$ , while  $m$  and  $s$  are intensities of  $M$  and  $S$  respectively. By approximation, the velocity can be expressed as:

$$\vec{v} = \frac{(m - s) \nabla s}{\|\nabla s\|^2} \quad (12)$$

Generally  $\vec{v}$  is considered simply as a displacement. Since equation (12) is unstable for small values of  $\nabla s$ , an additional term is added, which generates the equation (13).

$$\vec{v} = \frac{(m - s) \nabla s}{\|\nabla s\|^2 + (m - s)^2} \quad (13)$$

This algorithm is based on the implicit assumption that the intensities of two corresponding voxels are equal, and seeks to maximize the intensity similarity using the sum of squared difference between a source image and a target image. However this condition is seldom fulfilled in real-world medical image registration without intensity normalization, because there are many factors that may affect observed intensity of a tissue over the imaged field, such as the different scanner or scanning parameters, normal aging, different subjects, and so on. Another assumption in Demons registration is of a small deformation between the source image and the target image, which is also not true in inter-subject registration. Therefore, preprocessing before applying Demons registration is necessary. Or else, it might be failed or less effective when registering two subjects with large deformation and/or intensity differences [19][22][27]. For intensity normalization, a simple scaling of the intensities considering mean and standard deviation normalization often appears to be insufficient since the relationship between voxel intensities of two images can be non-linear, in particular when both images come from different scanners. So the commonly used preprocessing techniques are based on image histogram or joint histogram [19][20]. For spatial normalization, global rigid or affine transformation is often used as initialization of a following nonlinear registration [25]. Since it is difficult to estimate the geometric and intensity changes simultaneously, most preprocessing methods adjust shape and intensity respectively. However, a stepwise

adjustment influences each other as space normalization depends on the intensity consistency of the corresponding structures, while intensity normalization is also dependent on the spatial correspondence. Fortunately the adopted local affine transformation described in section 2.1 is more effective to deal with larger deformation and can modify simultaneously the geometric shape and brightness/contrast differences despite its limited ability in registering subtle deformation due to the necessary size of the subregions. Therefore, it is reasonable to combine the two registration algorithm to complete the segmentation task. After local affine transformation with adaptively intensity correction, the shape differences and the intensity variations between the reference image and the floating image will be small enough to satisfy the assumption of Demons algorithm. This enables the Demons registration algorithm more effectively to deal with subtle local differences.

### 3. Experiments and Results

Two experiments were carried out to assess the performance of the proposed segmentation method. The first was synthetic deformation experiment, in which the SPL [28] standard reference image (obtained from the Surgical Planning Laboratory of Harvard Medical School) and the corresponding atlas were deformed using an analytic harmonic deformation approach [29]. Then the reference image was registered to the deformed image to get the deformation field. Finally the acquired segmentation result using the deformation field was compared with the real segmentation, the deformed atlas. Ten volumes were used in this experiment. The second experiment consists of a segmentation performance comparison between the proposed method and public brain structures segmentation software, ITK-SNAP [30], using ten real data. ITK-SNAP provides semi-automatic segmentation using active contour methods, as well as manual delineation and image navigation. The mathematical theory behind snake evolution in SNAP and the user guide can be found in [30] and the website <http://www.itksnap.org/>, respectively. A number of steps requiring manual user input are described in the SNAP tutorial, including (1) choose the type of the feature image to be used, (2) select the parameters used to compute the feature image, (3) initialize the snake using spherical bubbles, and (4) choose the relative weights of the different types of velocities that drive snake evolution. In the experiment, those parameters are set carefully after adequate practices in order to ensure fair comparisons as far as possible.

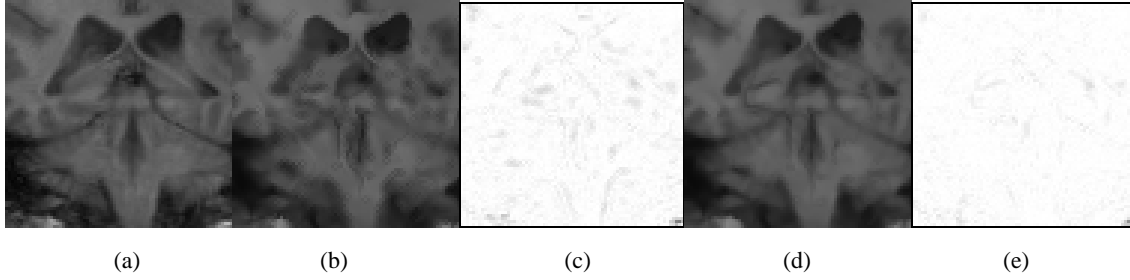
#### 3.1. Materials

The SPL reference image consists of  $256 \times 256 \times 160$  voxels with a spatial resolution of  $0.9375\text{mm} \times 0.9375\text{mm} \times 1.5\text{mm}$ . The test images were imaged with 1.5T GE scanner, and Axial 3D IR T1-weighted (TI/TR/TE: 600/10/2) acquired using a fast gradient echo with inversion recovery sequence. Each dataset (volume) consists of  $256 \times 256 \times 124$  voxels, and the resolution of each voxel is  $0.9375\text{mm} \times 0.9375\text{mm} \times 1.5\text{mm}$ . Both larger intensity difference between the reference image and the test image due to different scan equipment and the individual morphology differences between subjects can be observed, that makes the registration difficult.

#### 3.2. Results

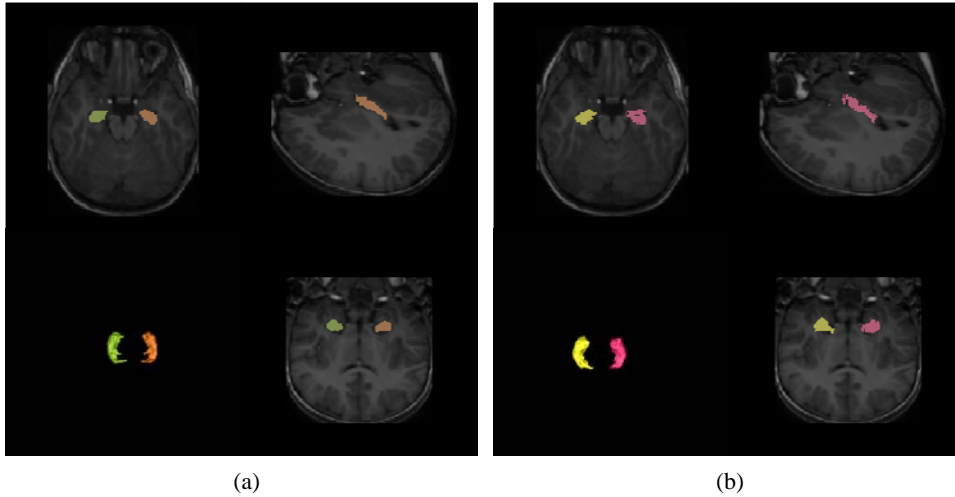
##### 3.2.1. Visual inspection and comparison

Figure 1 shows the registration performances before and after correcting subtle local differences using Demons registration. It can be seen that the difference is larger when only using local elastic registration (Figure 1(c)). After subtle local difference correction using Demons registration, the difference decreases.



**Fig. 1.** Comparison of the local elastic registration and the proposed method. (a) Internal region of reference image. (b) Result of local elastic registration. (c) Differences between (a) and (b). (d) Result of the proposed method. (e) Differences between (a) and (d).

Figure 2 shows the segmentation result using the proposed method. Visual inspection of the segmentation results was performed by comparing “gold standard” and automatic segmentation on the hippocampus. It can be seen that the automatic segmentation result is acceptable and encouraging.



**Fig. 2.** Comparison of “gold standard” and automatic segmentation on the hippocampus. (a) Manual segmentation by expert (b) Automatic segmentation using the proposed method.

### 3.2.2. Quantitative evaluation

**Validation criteria.** To validate the results quantitatively, the criteria widely used in atlas-based segmentation [1][2][3][14][19], a kappa statistic based similarity index (KI) is adopted in this paper. The KI value measures the overlap ratio between the segmented structure and the ground truth, which is defined as  $KI = 2TP / (2TP + FN + FP)$ . The definitions of the parameters are as follows:  $TP = G \cap E$  is the number of true positive;  $FP = \bar{G} \cap E$  is the number of false positive and  $FN = G \cap \bar{E}$  is the number of false negative. Where  $G$  is the true segmentation of a given structure,  $E$  is the estimated segmentation of the same structure, and  $\bar{A}$  denotes the complement of a set  $A$ .

**Validation using synthetic deformation.** Since it is hard to obtain real MRI images of the human brain with known segmentation results of the internal structures, a quantitative assessment of the performance of the segmentation method requires the use of simulated data with known segmentation as the gold standard. The synthetic images came from the deformed SPL reference image, which was deformed using an analytic harmonic deformation approach [29].

Table 1 shows the segmentation results on simulated data. It can be seen that there were great differences in cross correlation between the deformed images and the original reference image by the synthetic deformation. However the

mean  $KI \pm \text{standard deviation}$  for ten cases was  $0.9927 \pm 0.0075$  which was perfect results regardless how low the cross correlation was before registration between the reference image and the floating image. It showed that high registration quality could lead to high segmentation results.

**Validation with expert delineation.** Although validation with simulated data is a common method for its known segmentation, it is not sufficient to validate the approach. One drawback is that the deformation is not representative of the real inter-subject variability, and the other is that it doesn't consider the noise and artifact in real MRI images. So additional testing with real data must also be completed to demonstrate the ability of the algorithm to work under real-world conditions. For this reason, several real MRI data from different subjects were also used to test the performance of the approach. Table 2 shows the segmentation result using real brain MRI data. For the results using ITK-SNAP software, the best overlap ratio was 0.6814 and the worst was 0.4281, and the mean $\pm$ standard deviation was  $0.5811 \pm 0.0597$  for ten cases. For the results using the proposed method, the best overlap ratio was 0.8636 and the worst was 0.6592, and the mean $\pm$ standard deviation was  $0.7749 \pm 0.0564$ . The results show that the proposed method is superior to the ITK-SNAP in hippocampus segmentation. Since ITK-SNAP uses active surface methods implemented in a level-set framework, the final segmentation depends to some extent on the starting position of the active surface. Also because the deforming surface is driven by an intensity-based energy minimization function, it is difficult to segment the hippocampus due to the lack of local intensity information to determine the hippocampal boundary.

**Table 1.** Segmentation results on simulated data using the proposed method

Volume	Cross Correlation		KI value	
	<i>before</i>	<i>after</i>	<i>Left</i>	<i>Right</i>
1	0.5700	1	0.9762	0.9756
2	0.6339	1	0.9922	0.995
3	0.6583	1	0.9941	0.9928
4	0.7173	1	0.9867	0.9871
5	0.7499	1	0.9902	0.9875
6	0.7573	1	0.9889	0.9921
7	0.8238	1	0.9965	1
8	0.9421	1	1	1
9	0.9555	1	1	1
10	0.9738	1	1	1

**Table 2.** Comparison of KI values on real data between ITK-SNAP software and the proposed method

Method	Volume	1	2	3	4	5	6	7	8	9	10
Proposed	<i>Left</i>	0.8636	0.7351	0.8075	0.8555	0.8155	0.7543	0.7502	0.7630	0.8299	0.8431
	<i>Right</i>	0.7410	0.7722	0.6592	0.8207	0.7359	0.7807	0.6621	0.8026	0.7427	0.7639
SNAP	<i>Left</i>	0.6814	0.6085	0.6135	0.6236	0.5390	0.5928	0.4546	0.5540	0.6577	0.6270
	<i>Right</i>	0.5471	0.5718	0.5594	0.6155	0.5675	0.6015	0.4281	0.5916	0.6036	0.5835

## 4. Discussion

Two validation methods were used in this paper to evaluate the segmentation ability of the proposed non-rigid registration approach. The first was on the simulated data with known segmentation acquired from the synthetic

deformation, while the second was on real data with the expert delineation. Each validation method show their advantages and disadvantages. Validation on simulated data makes it possible generate known reference segmentation, thus the accuracy of the estimated solution can be evaluated. However there exist two main drawbacks. One is that the deformation is not representative of the real intersubject variability and the other is that it doesn't consider the noise and artifact in real MRI images. The second validation method is obviously in line with the actual situation. The main drawback of this validation is that the segmentation map, provided by an expert, cannot be considered as a perfect ground truth. So it can be seen that the first validation method has true reference segmentation but is not representative of the real situation, while the second validation method reflects the real situation but has no completely true reference segmentation. From the two experiment results, a phenomenon was also worthy of paying attention to. The segmentation result is very nice on simulated data. While the segmentation result on real data is relatively not good enough. It is possible that using expert segmentation as gold standard may have influence on the result, but it should not be the main reason. The actual reason should be due to the data differences. As it can be seen there are two main differences between the two data. One is that the deformation in simulated data couldn't reflect the real shape difference in different subjects while the real data could. However both the deformation are nonlinear, they should have the same characteristic. Thus it should not be the main reason. The other difference is that for simulated data, the homologous structures in reference image and floating image have the similar intensity. But for real data, these are not true because of the noise and interference introduced by the scanning procedure. This should be a serious problem for intensity based registration. The obtained better results using the proposed method have provided some evidences. Therefore, improving image quality and intensity correspondence of homologous structures should be a promising strategy for structure segmentation based on intensity based non-rigid registration.

## **5. Conclusion**

A combination of local affine transformation and Demons free-form transformation is used to segment the hippocampus automatically in this paper. The segmentation results on both the simulated data and the real data are encouraging. It indicates that the proposed method could be a solution for segmenting such brain internal structures which lack clearly defined intensity boundaries from human MRI images. Compared to global affine transform and simple histogram match, the selected local affine transform with intensity correction simultaneously provide a better initial conditions to the Demons registration algorithm. Furthermore, the results on the simulated data are superior to that on the real data due to the nice intensity correspondence between the homologous structures. It can be concluded that the image gray level of the corresponding structures plays an important role in registration based segmentation using intensity metric.

## **6. Acknowledgments**

This work is partly supported by National Science Foundation of China (No.30570475, No. 60372081, No.60872122) and the Youth Foundation of Dalian University of Technology, China.

## 7. References

- [1] B. M. Dawant, S. L. Hartmann, J. -P. Thirion, *et al.* Automatic 3-D Segmentation of Internal Structures of the Head in MR Images Using a Combination of Similarity and Free-Form Transformations: Part I, Methodology and Validation on Normal Subjects. *IEEE Transactions On Medical Imaging*, 1999, 18(10): 909–916.
- [2] Bruce Fischl, David H. Salat, Evelina Busa, *et al.* Whole Brain Segmentation: Automated Labeling of Neuroanatomical Structures in the Human Brain. *Neuron*, 2002, 33(1): 341–355.
- [3] Yan Xia, Keith Bettinger, Lin Shen, Allan L. Reiss. Automatic Segmentation of the Caudate Nucleus From Human Brain MR Images. *IEEE Transactions on Medical Imaging*, 2007, 26(4): 509–517.
- [4] J. Barnes, J. Foster, R.G. Boyes, T. Pepple, E.K. Moore, J.M. Schott, C. Frost, R.I. Scahill, and N.C. Fox. A comparison of methods for the automated calculation of volumes and atrophy rates in the hippocampus. *NeuroImage* 40 (2008) 1655 - 1671.
- [5] Killiany, R.J., Hyman, N., Gomez-Isla, T., 2002. MRI measures of entorhinal cortex vs hippocampus in preclinical AD. *Neurology* 58, 1188 - 1196.
- [6] Xu, Y., Jack Jr., C.R., O' Brien, P.C., Kokmen, E., Smith, G.E., Ivnik, R.J., Boeve, B.F., Tangalos, R.G., Petersen, R.C., 2000. Usefulness of MRI measures of entorhinal cortex versus hippocampus in AD. *Neurology* 54, 1760 - 1767.
- [7] M. G. Linguraru, M. Á. G. Ballester, N. Ayache. Deformable Atlases for the Segmentation of Internal Brain Nuclei in Magnetic Resonance Imaging. *International Journal of Computers, Communications & Control*, 2007(II): 26–36.
- [8] Chan, D., Fox, N.C., Scahill, R.I., Crum, W.R., Whitwell, J.L., Leschziner, G., Rossor, A.M., Stevens, J.M., Cipelotti, L., Rossor, M.N., 2001. Patterns of temporal lobe atrophy in semantic dementia and Alzheimer' s disease. *Ann. Neurol.* 49, 433 - 442.
- [9] L. Clarke, R. Velthuizen, M. Camacho, *et al.* MRI segmentation: Methods and applications. *Magn. Resonance Imag.*, 1995, 13: 343–368.
- [10] T. McInerney D. Terzopoulos. Deformable models in medical image analysis: A survey. *Med. Image Anal.*, 1996, (1): 91–108.
- [11] P. Yushkevich, J. Piven, H. Hazlett, R. *et al.* User-guided 3-D active contour segmentation of anatomical structures: Significantly improved efficiency and reliability. *NeuroImage*, 2006, 31: 1116–1128.
- [12] Pitiot, H. Delingette, P. Thompson, N. Ayache. Expert knowledge-guided segmentation system for brain MRI. *NeuroImage*, 2004, 23: 85–96.
- [13] T. F. Cootes, A. Hill, C. J. Taylor, J. Haslam. The use of active shape models for locating structures in medical images. *Image and Vision Computing*, 1994, 12(6): 355–366.
- [14] C. Baillard, P. Hellier, C. Barillot. Segmentation of brain 3D MR images using level sets and dense registration. *Medical Image Analysis*, 2001, 5: 185–194.
- [15] Daniel Schwarz, Tomas Kasperek, Ivo Provaznik, Jiri Jarkovsky. A Deformable Registration Method for Automated Morphometry of MRI Brain Images in Neuropsychiatric Research. *IEEE Transactions on Medical Imaging*, 2007, 26(4): 452–461.
- [16] D. V. Iosifescu, M. E. Shenton, S. K. Warfield, *et al.* An automated registration algorithm for measuring MRI subcortical brain structures. *NeuroImage*, 1997, 6: 13–25.
- [17] A. Kelemen, G. Szekely, and G. Gerig. Elastic model-based segmentation of 3-D neuroradiological data sets. *IEEE Trans. Med. Imag.*, 1999, 18(10): 828–839.
- [18] J. P. Thirion. Image matching as a diffusion process: an analogy with Maxwell's demons. *Medical Image Analysis*, 1998, 2(3): 243–260.
- [19] V. Noblet, C. Heinrich, F. Heitz, *et al.* Retrospective evaluation of a topology preserving non-rigid registration method. *Medical Image Analysis*, 2006, 10: 366–384.
- [20] Alexandre Guimond, Alexis Roche, Nicholas Ayache, *et al.* Three-Dimensional Multimodal Brain Warping Using the Demons Algorithm and Adaptive Intensity Corrections. *IEEE Transactions On Medical Imaging*, 2001, 20(1): 58–69.
- [21] He Wang, Lei Dong, *et al.* Validation of an accelerated 'demons' algorithm for deformable image registration in radiation

therapy. *Phys. Med. Biol.*, 2005, 50(12): 2887–2905.

- [22] M. Bach Cuadra, M. De Craene, V. Duay, *et al.* Dense deformation field estimation for atlas-based segmentation of pathological MR brain images. *Computer Methods And Programs In Biomedicine*, 2006, 84: 66–75.
- [23] P. Hellier\*, C. Barillot, I. Corouge, *et al.* Retrospective Evaluation of Intersubject Brain Registration. *IEEE Transactions on Medical Imaging*, 2003, 22(9): 1120–1130.
- [24] Parraga A, Susin A, Pettersson J, Macq B, De Craene M. Quality Assessment of Non-rigid Registration Methods for Atlas-based Segmentation in Head-neck Radiotherapy. *Proceedings of IEEE International Conference on Acoustics, Speech, & Signal Processing*, Honolulu, Hawaii, USA, 2007. Volume: 1, I-445–I-448.
- [25] Arno Klein, Jesper Andersson, Babak A. Ardekani, John Ashburner, *et al.* Evaluation of 14 nonlinear deformation algorithms applied to human brain MRI registration, *NeuroImage* **46** (2009), pp. 786–802.
- [26] Senthil Periaswamy, Hany Farid. Elastic Registration in the Presence of Intensity Variations. *IEEE Transactions on Medical Imaging*, 2003, 22(7): 865–874.
- [27] Cuadra M.B., Cuisenaire O., Meuli R., *et al.* Automatic segmentation of internal structures of the brain in MR images using a tandem of affine and non-rigid registration of an anatomical brain atlas, *Proceedings of 2001 International Conference on Image Processing* **3** (2001), 1083-1086.
- [28] R. Kikinis, *et al.* A digital brain atlas for surgical planning, model driven segmentation and teaching, *IEEE Trans. Visual. Comput. Graph.* 1996, 2 (3):232–241.
- [29] Weiguo Lu, *et al.* Fast free-form deformable registration via calculus of variations. *Phys. Med. Biol.* 2004, 49: 3067–3087.
- [30] Paul A. Yushkevich, Joseph Piven, Heather Cody Hazlett, Rachel Gimpel Smith, Sean Ho, James C. Gee, and Guido Gerig. User-guided 3D active contour segmentation of anatomical structures: Significantly improved efficiency and reliability. *Neuroimage*, 2006, 31(3):1116-28.